COBEM UBERLÂNDIA 2019

ABCM Associação Brasileira de Engenharia e Ciências Mecânicas

25th ABCM International Congress of Mechanical Engineering
October 20-25, 2019, Uberlândia, MG, Brazil

Dissipated energy analysis of aeroelastic system with nonlinear stiffness with application to energy harvesting

Ana Carolina Godoy Amaral
Marcos Silveira
São Paulo State University - UNESP, Bauru - SP
Av. Engenheiro Luiz Edmundo Carrijo Coube, 14-01, CEP: 17033-360 - Vargem Limpa, Bauru - SP
ana.carolina@unesp.br, marcos.silveira@unesp.br

Abstract. *The main objective of energy harvesting is to capture the energy present in the environment and transfer it to the various available electronic devices. The objective of this research project is to study the dynamic behavior of an energy harvesting system using a piezoelectric transducer applied to an aeronautical structure in flutter condition, with nonlinear stiffness. The mathematical model for dynamic analysis of a flexible wing structure under forcing conditions described will be analysed through numerical simulation. The influence of nonlinear stiffness in the system is analysed by quantifying the mechanical and electrical power in the system. Also, the influence of nonlinear terms on the flutter speed is studied.*

Keywords: *nonlinear stiffness, energy harvesting, piezoeletric transducer, flutter*

1. INTRODUCTION

Energy harvesting is attracting much interest and many applications are being developed related to aeroelastic systems. This technology has as main objective to capture the kinetic energy present in the environment and transfer it to available electronic devices. It can be applied to structural vibration, vehicle dynamics or human movement itself. One of the fields of study where energy harvesting can be applied is in aeronautics, where it can remove energy from the mechanical oscillations, consequently increasing the flutter speed. Harb (2011) shows the current state of the energy harvesting concept. The first observation of harvesting energy was in 1880 with Pierre and Jacques Currie. Since then, interest in this technology has resulted in some applications, such as MEMS (micro electromechanical systems), and energy harvesting from human movements. Thus, studying ways to increase efficiency of energy harvesting is very important because the higher the energy, the more interesting this type of technology can be for society. Ghandchi-Tehrani and Elliott (2014) showed that it is possible to increase the energy harvesting dynamic range by introducing nonlinear damping, in this case with a cubic term. The power is measured with several different parameters, so it is perceived that the power captured with the nonlinear damping is greater than that captured with the linear damping, when in resonance, at an excitation below its maximum excitation. The use of intelligent materials in aeronautical problems has been a tendency in the present days. Marqui Jr *et al.* (2005) created a flexible assembly system, which represents a dynamic system of two degrees of freedom, pitch and plunge, in which a rigid wing encounters classic flutter vibration in a wind tunnel. A mathematical model is proposed to gain insight into system operation, and can later work with flutter suppression, and keep the system stable over a wide range of test speeds. The results obtained shows that controllers are able to control complex phenomena such as flutter. Sousa *et al.* (2017) employs a Synchronized Switch Damping on Inductor (SSDI) technique, which is capable of dealing with the nonlinear characteristics of the electrical domain of the problem, and the use of shape memory alloys (SMA) as an alternative to conventional actuators. The nonlinearity applied to the system by the SMA and SSDI together results in better aeroelastic behaviour, so stable LCOs (limited cicle oscillations) of acceptable amplitudes are obtained for a range of velocities 25 % higher than in a linear system. It is clear that changing some factors of the system will make it behave in different ways, bringing new possibilities, when working with aeroelastic systems and flutter. In order to explore further the role of nonlinearities on the energy harvesting and flutter suppression, the objective of this work is to study the dynamic behaviour of an energy harvesting system using a piezoelectric transducer applied to an aeronautical structure in flutter condition, with nonlinear stiffness.

2. AEROELASTIC TYPICAL SECTION FOR WIND ENERGY HARVESTING

Figure 1 shows the model of the typical section studied. The system presents piezoelectric associated to plunge movement and nonlinear stiffness of the cubic type associated to plunge movement. The dynamical equations of this

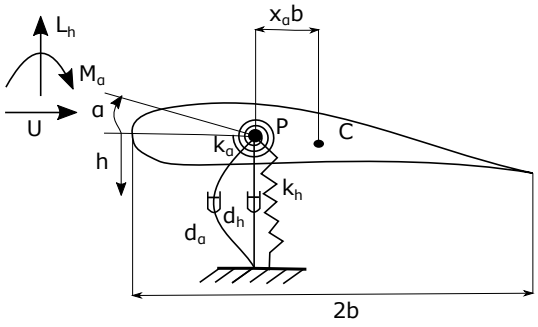

Figure 1. Aeroelastic section under wind excitation.

nonlinear model, in dimensionless form, are:

$$\begin{aligned}\beta\overline{h}'' + x_\alpha\alpha'' + \zeta_h\overline{h}' + \overline{h} + \delta\overline{h}^3 - \kappa\overline{v} &= -L_h \\ x_\alpha\overline{h}'' + \overline{r}_\alpha^2\alpha'' + \zeta_\alpha\alpha' + \gamma^2\overline{r}_\alpha^2\alpha &= M_\alpha \\ \eta\overline{v}' + \frac{\overline{v}}{\lambda} + \kappa\overline{h}' &= 0\end{aligned} \tag{1}$$

in which $\overline{h}$ and α are the dimensionless plunge and pitch displacements, β is the dimensionless mass ratio, ζ_h and ζ_α are the dimensionless plunge and pitch damping ratios, x_α is the dimensionless chord-wise offset of the elastic axis from the centroid, $\overline{r}_\alpha$ is the dimensionless radius of gyration, γ is the dimensionless frequency ratio, M_α is the dimensionless aerodynamic moment, L_h is the dimensionless aerodynamic lift, δ is the dimensionless nonlinear stiffness coefficient, κ is the dimensionless electromechanical coupling, λ is the dimensionless load resistance, $\overline{v}$ is the dimensionless electrical voltage, η is the dimensionless equivalent capacitance, and $'$ denotes differentiation over dimensionless time (τ). Note that the system without the piezoelectric transducer is obtained by the first two equations and without the coupling term κ in the first equation. The definition of the dimensionless terms are given by Marqui Jr and Erturk (2013).

Equations for the aerodynamic loads are from a quasi-static aerodynamic system for lift (L) and moment (M) given by Dimitriadis (2017) and reproduced here:

$$\begin{aligned}L &= \rho\pi b^2\left(\ddot{h} - \left(x_f - \frac{c}{2}\right)\ddot{\alpha}\right) + \rho\pi b^2 U\dot{\alpha} + \rho U^2 c\pi\left(\alpha + \frac{\dot{h}}{U} + \left(\frac{3}{4}c - x_f\right)\frac{\dot{\alpha}}{U}\right) \\ M &= \rho\pi b^2\left(x_f - \frac{c}{2}\right)\left(\ddot{h} - \left(x_f - \frac{c}{2}\right)\ddot{\alpha}\right) - \frac{\rho\pi b^4}{8}\ddot{\alpha} - \left(\frac{3}{4}c - x_f\right)\rho\pi b^2 U\dot{\alpha} \\ &\quad + \rho U^2 e c^2\pi\left(\alpha + \frac{\dot{h}}{U} + \left(\frac{3}{4}c - x_f\right)\frac{\dot{\alpha}}{U}\right) - \frac{1}{16}\rho U c^3\pi\dot{\alpha}\end{aligned} \tag{2}$$

in which ρ is the density, b is the half length of the airfoil, x_f is the distance from the beginning of the aerofoil to the torsion center, c is the length of the airfoil, U is the wind speed, and $e = x_f/c - 1/4$. Note that Eq. (2) is not in the dimensionless form. To include them in Eq. (1), we use $L_h = L/mb\omega_h^2$ and $M_\alpha = M/mb^2\omega_h^2$. Also, the dimensionless speed equation is given by $\overline{U} = U/\omega_h b$ (Marqui Jr and Erturk, 2013).

Another way to represent Eq.(1) is in the matrix form proposed by Edwards (1979). In this formulation, the state variables are h, α, h', α', x_1, x_2, v with $x_a = [x_1 \quad x_2]^t$ being the augmented aerodynamical states (Edwards, 1979). Also, electromechanical coupling must be included in the matrix formulation (Marqui Jr and Erturk, 2013). The dynamical equations of this model including nonlinear stiffness, in the matrix form, are:

$$\begin{bmatrix} I & 0 & 0 & 0 \\ 0 & \tilde{M} & 0 & 0 \\ 0 & 0 & I & 0 \\ 0 & 0 & 0 & \eta \end{bmatrix}\begin{bmatrix} x' \\ x'' \\ x_a' \\ \overline{v}' \end{bmatrix} = \begin{bmatrix} 0 & I & 0 & 0 \\ -\tilde{K} & -\tilde{B} & D & \theta_1 \\ E_1 & E_2 & F & 0 \\ 0 & -\theta_2 & 0 & -\frac{1}{\lambda_l} \end{bmatrix}\begin{bmatrix} x \\ x' \\ x_a \\ \overline{v} \end{bmatrix} + g(x, x', x_a, \overline{v}) \tag{3}$$

in which $\theta_1 = [0 \quad \kappa]^t$, $\theta_2 = [0 \quad \kappa]$, $x = [a \quad \overline{h}]^t$, $x_a = [x_1 \quad x_2]^t$, I is the 2x2 identity matrix, $\tilde{M}$, $\tilde{B}$, $\tilde{K}$ are calculated through the respective structural mass, damping and stiffness matrices. $\tilde{M}$, $\tilde{B}$, $\tilde{K}$ and the aerodynamic matrices D, E_1, E_2, F can be found in (Edwards, 1979) and $g(x, x', x_a, \overline{v})$ is the vector with nonlinear terms.

In order to analyse the influence of nonlinear stiffness, the average power per cycle is calculated for the mechanical and electrical domains. The instantaneous power dissipated by the mechanical system related to plunge and pitch and the

instantaneous electrical power are given by:

$$P_h = \zeta_h \overline{h}'^2 \qquad P_\alpha = \zeta_\alpha \alpha'^2 \qquad P_e = \overline{v}^2/\lambda \tag{4}$$

With the instantaneous power calculated, it is possible to calculate the average power per cycle, $\overline{P_h}$, $\overline{P_\alpha}$ and $\overline{P_e}$ (Stephen, 2006).

3. FLUTTER SPEED DETERMINATION

For the linear system, the flutter speed was calculated through analytical stability analysis. For the nonlinear system, it was calculated through numerical simulation, where a sequential search was performed. From a initial guess, and with the other parameters fixed, U was increased until two consecutive peaks have same value, indicating the presence of a LCO. This can been interpreted as an optimization problem with the objective function given by equation:

$$f(x) = |D| - E \tag{5}$$

in which D is the difference between the penultimate peak and last peak, and E is a tolerance. Equation (5) allows the reasoning that in order for flutter to happen, the distance between the peaks must be 0. Since the equations are solved numerically, a tolerance must be considered.

3.1 Flutter speed variation as a function of the electromechanical coupling

The section represented by Fig.1, with linear piezoelectric, was studied using aerodynamic models from (Edwards, 1979) and from (Dimitriadis, 2017). For both cases, an analytical simulation and an numerical simulation was performed. For (Edwards, 1979) aerodynamic model, the following parameters were adopted: $\beta = 2.5940$, $\overline{r}_\alpha = 0.5467$, $\gamma = 0.5090$, $\zeta_h = 0.0535$, $\zeta_\alpha = 0.1102$, $x_\alpha = 0.25$, $\rho = 1.2754$ kg/m^3, $b = 0.76$ m, κ ranges from 2×10^{-6} to 10×10^{-6}, $n = 3.66 \times 10^{-9}$, $\lambda = 0.48 \times 10^9$, $x_f = b - x_\alpha b$, $c = b/2$, $m = 92.53$ kg, $\omega_h = 50$ rad/s, $a = -0.4$ and $\mu = 40$. The initial conditions used in all simulations were: $\overline{h} = 0.1$, $\alpha = 0.1$, $\overline{h}' = 0$, $\alpha' = 0$, $x1 = 0.1$, $x2 = 0.1$, $\overline{v} = 0$.

For Dimitriadis (2017) aerodynamic model, the following parameters were adopted: $\beta = 2.5940$, $\overline{r}_\alpha = 0.5467$, $\gamma = 0.5090$, $\zeta_h = 0.0535$, $\zeta_\alpha = 0.1102$, $x_\alpha = 0.25$, $\rho = 1.2754$ kg/m^3, $b = 0.76$ m, κ ranges from 2×10^{-6} until 10×10^{-6}, $n = 3.66 \times 10^{-9}$, $\lambda = 0.48 \times 10^9$, $x_f = b - x_\alpha b$, $c = b/2$, $m = 92.53$ kg and $\omega_h = 50$ rad/s. The initial conditions used in all simulations were: $\overline{h} = 0.1$, $\overline{h}' = 0$, $\alpha = 0.1$, $\alpha' = 0$, $\overline{v} = 0$.

Figure 2 shows the variation of the flutter speed as a function of the electromechanical coupling for the aerodynamic model from Dimitriadis (2017), and for the aerodynamic model from Edwards (1979). The difference between the numerical and analytical solutions for the aerodynamic model from Dimitriadis (2017), it's smaller than 2×10^{-3}, while for the aerodynamic model from Edwards (1979) it's smaller than 3×10^{-3}. The major difference between Dimitriadis (2017) and Edwards (1979) is given by lower values of κ, for example $\kappa = 2 \times 10^{-6}$, the difference is 0.038, for numerical solution and 0.037, for analytical solution.

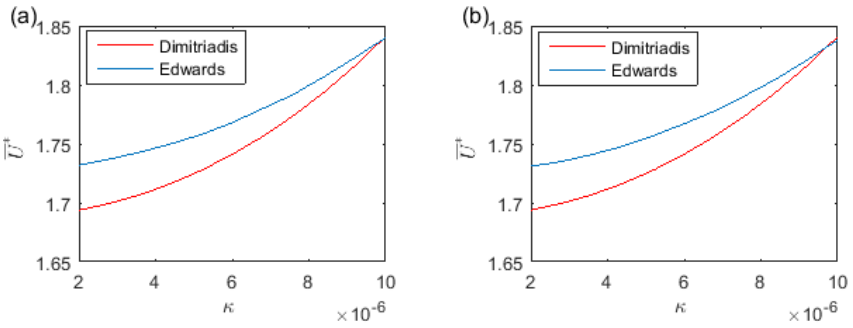

Figure 2. Flutter speed as a function of the electromechanical coupling, (a) for aerodynamic models from Dimitriadis (2017) and from Edwards (1979) by the fourth order runge kutta method, (b) for aerodynamic models of Dimitriadis (2017) of Edwards (1979) by calculating the eigenvalues.

3.2 Flutter speed as a function of electromechanical coupling and electrical resistance

For the flutter speed as a function of the electromechanical coupling, we fixed $\lambda = 0.48 \times 10^9$ and κ ranges from 2×10^{-6} to 8×10^{-6}. For the flutter speed as a function of the electrical resistance, we fixed $\kappa = 8 \times 10^{-6}$ and λ ranges from 0.1×10^9 to 2×10^9. For the nonlinearity $\delta = 10$. Figure 3 shows flutter speed as a function of the electromechanical coupling, and of the electrical resistance coupling of the system with 3 degrees of freedom (with piezoelectric).

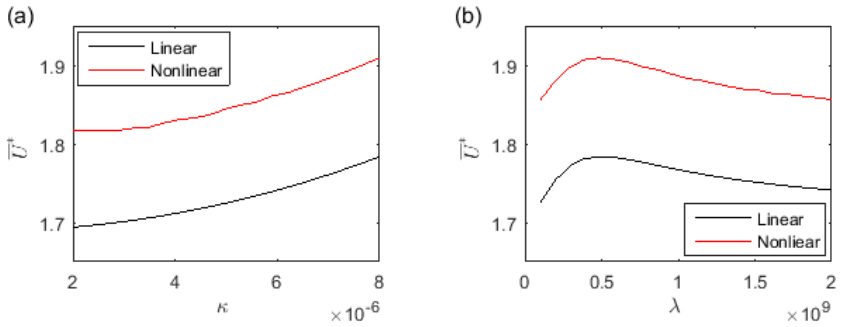

Figure 3. (a) Flutter speed as a function of the electromechanical coupling, (b) Flutter speed as a function of the electrical resistance.

Flutter speed increases, if the electromechanical coupling is increased, and for the electrical resistance, flutter speed has his maximum around 0.5×10^9. It can be stated that the nonlinearity increases the flutter speed.

3.3 Velocity related to plunge as a function of time

For $\lambda = 0.48 \times 10^9$, we used $\kappa = 3 \times 10^{-6}$, and $\kappa = 7 \times 10^{-6}$. For $\kappa = 8 \times 10^{-6}$, we used $\lambda = 0.5 \times 10^9$, and $\lambda = 1.5 \times 10^9$. Figures 4, 5, 6, 7 shows velocity related to plunge as a function of time of a system with 3 degrees of freedom (with piezoelectric), with $\kappa = 3 \times 10^{-6}$, $\kappa = 7 \times 10^{-6}$, $\lambda = 0.5 \times 10^9$, and $\lambda = 1.5 \times 10^9$. The difference between the amplitude is smaller than 3×10^{-3}, for the first case, smaller than 5×10^{-3}, for the second case, and smaller than 2.5×10^{-3}, for the third case and the fourth case, knowing that the nonlinear section has the bigger amplitude.

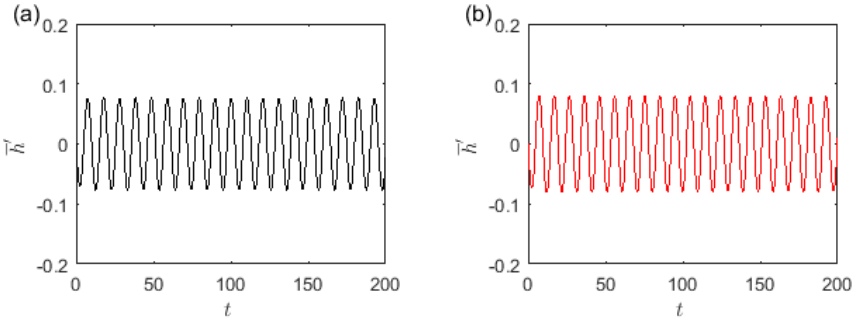

Figure 4. Velocity related to plunge as a function of time, with $\kappa = 3 \times 10^{-6}$ (a) in a linear section, (b) in a nonlinear section, with $\delta = 10$.

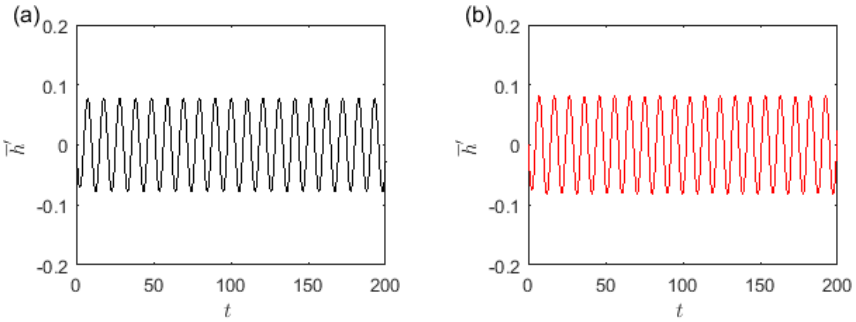

Figure 5. Velocity related to plunge as a function of time, with $\kappa = 7 \times 10^{-6}$ (a) in a linear section, (b) in a nonlinear section, with $\delta = 10$.

3.4 Electrical voltage as a function of time

Figure 8, 9, 10, 11 shows electrical voltage as a function of time of a system with 3 degrees of freedom (with piezoelectric), with $\kappa = 3 \times 10^{-6}$, $\kappa = 7 \times 10^{-6}$, $\lambda = 0.5 \times 10^9$, and $\lambda = 1.5 \times 10^9$. The difference between the amplitude is smaller than 1.5, for the first case, smaller than 6, for the second case, smaller than 3, for the third case, smaller than 2, for the fourth case, knowing that the nonlinear section has the bigger amplitude.

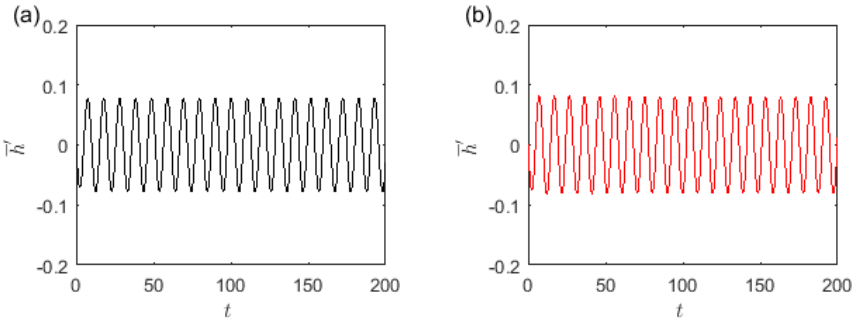

Figure 6. Velocity related to plunge as a function of time, with $\lambda = 0.5 \times 10^9$ (a) in a linear section, (b) in a nonlinear section, with $\delta = 10$.

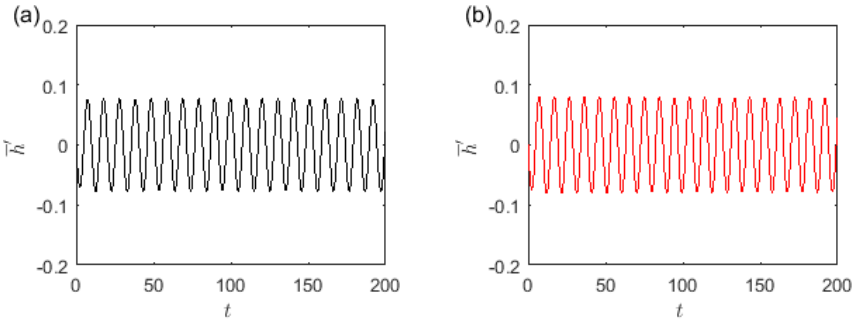

Figure 7. Velocity related to plunge as a function of time, with $\lambda = 1.5 \times 10^9$ (a) in a linear section, (b) in a nonlinear section, with $\delta = 10$.

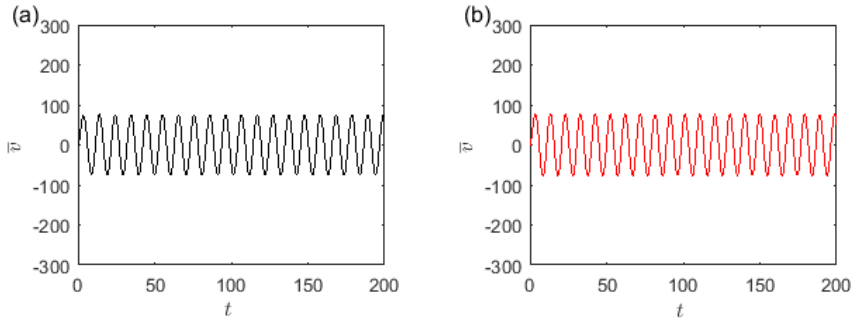

Figure 8. Electrical voltage as a function of time, with $\kappa = 3 \times 10^{-6}$ (a) in a linear section, (b) in a nonlinear section, with $\delta = 10$.

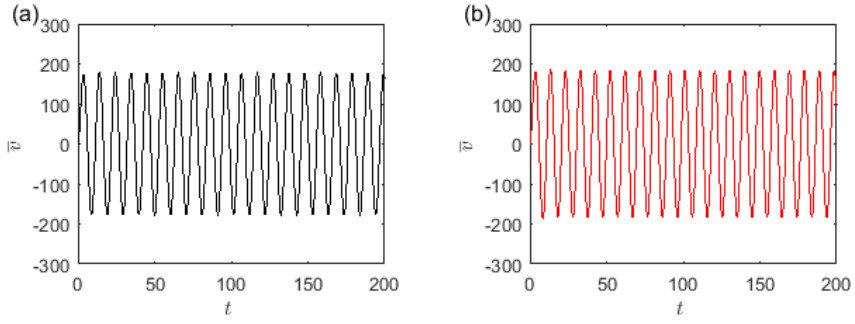

Figure 9. Electrical voltage as a function of time, with $\kappa = 7 \times 10^{-6}$ (a) in a linear section, (b) in a nonlinear section, with $\delta = 10$.

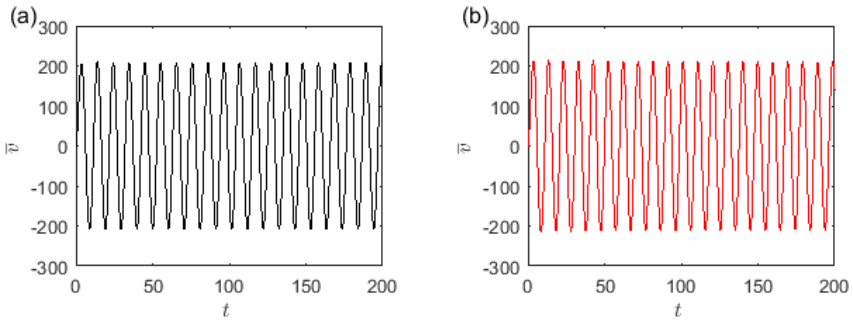

Figure 10. Electrical voltage as a function of time, with $\lambda = 0.5 \times 10^9$ (a) in a linear section, (b) in a nonlinear section, with $\delta = 10$.

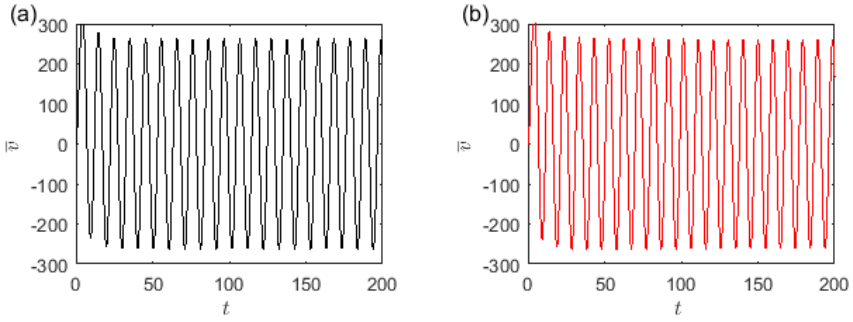

Figure 11. Electrical voltage as a function of time, with $\lambda = 1.5 \times 10^9$ (a) in a linear section, (b) in a nonlinear section, with $\delta = 10$.

The model with nonlinear term has higher amplitude of the velocity related to plunge and of the electrical voltage, being able to prove that the nonlinearity has influence at flutter speed and at electrical power.

4. MECHANICAL AND ELECTRICAL POWER

In this section the model represented by Fig.1 and by Eq.(1) is used. To study its dynamical behaviour, we obtain numerical solutions using the fourth order Runge-Kutta-Fehlberg method. The following parameters were adopted, adapted from Marqui Jr and Erturk (2013); Sousa *et al.* (2011): $\beta = 2.5940$, $\overline{r}_\alpha = 0.5467$, $\gamma = 0.5090$, $\zeta_h = 0.0535$, $\zeta_\alpha = 0.1102$, $x_\alpha = 0.25$, $\rho = 1.2754$ kg/m^3, $b = 0.76$ m, $\kappa = 5\times10^{-6}$, $n = 3.66\times10^{-9}$, $\lambda = 0.48\times10^9$, $x_f = b - x_\alpha b$, $c = b/2$, $m = 92.53$ kg, $\omega_h = 50$ rad/s and $\delta = 10$. The initial conditions used in all simulations were: $\overline{h} = 0.1$, $\overline{h}' = 0$, $\alpha = 0.1$, $\alpha' = 0$, $\overline{v} = 0$.

The dimensionless flutter speed $\overline{U}^*$ found, for the linear section and without piezoelectric transducer, was $\overline{U}^* = 1.6915$, for the linear section with piezoelectric transducer was $\overline{U}^* = 1.7247$, for the nonlinear section without piezoelectric transducer was $\overline{U}^* = 1.8112$ and for the nonlinear section with piezoelectric transducer was $\overline{U}^* = 1.8446$, showing that $\overline{U}^*$ with piezoelectric transducer was greater than the $\overline{U}^*$ without piezoelectric transducer in the linear and nonlinear systems. Figure 12 shows the average power as a function of $\overline{U}$. $\overline{P_h} = 1.975 \times 10^{-4}$, when in flutter, and $\overline{P_\alpha} = 3.735 \times 10^{-4}$ in the linear system without piezoelectric. For the linear system with piezoelectric, $\overline{P_h} = 1.586 \times 10^{-4}$, when in flutter, and $\overline{P_\alpha} = 2.937 \times 10^{-4}$. $\overline{P_e} = 1.654 \times 10^{-5}$. Similar analysis for the system with nonlinear stiffness is shown in Fig. 13. $\overline{P_h} = 1.774 \times 10^{-4}$ when in flutter, and $\overline{P_\alpha} = 3.076 \times 10^{-4}$ in the nonlinear system without piezoelectric. For the nonlinear system with piezoelectric, $\overline{P_h} = 1.671 \times 10^{-4}$, when in flutter, and $\overline{P_\alpha} = 2.838 \times 10^{-4}$. $\overline{P_e} = 1.648 \times 10^{-5}$, that is, $\overline{P_\alpha}$ is greater than $\overline{P_h}$ at flutter, and $\overline{P_e}$ is smaller than the other powers since it is withdrawn from the $\overline{P_h}$, for both cases. The application of non-linearity decreases electrical power collected from energy harvesting in 0.036%.

4.1 Variation of mechanical and electrical power as a function of the electromechanical coupling

Figure 14 shows mechanical power related to pitch and related to plunge as a function of the electromechanical coupling of the system with 3 degrees of freedom (with piezoelectric), for linear section and for nonlinear section ($\delta = 10$).

Figure 15 shows electrical power as a function of the electromechanical coupling of the system with 3 degrees of freedom (with piezoelectric), for linear section and for nonlinear section ($\delta = 10$).

For the mechanical power related to plunge as a function of electromechanical coupling we have an increase when we compare the linear section and the nonlinear section with $\delta = 10$. For the mechanical power related to pitch as a function

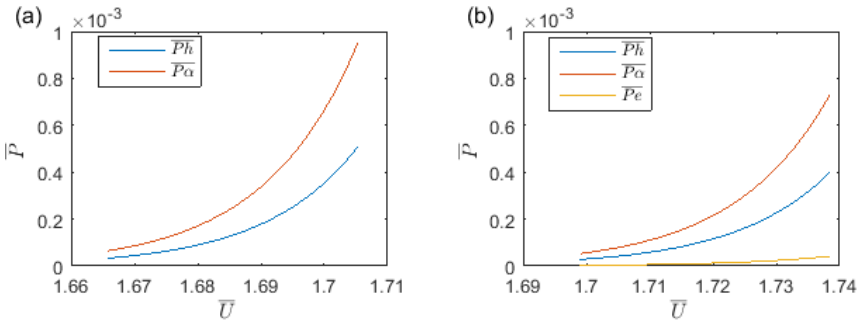

Figure 12. (a) $\overline{P_h}$ and $\overline{P_\alpha}$, for an aerolastic section with 2 DOF, without piezoelectric coupling, (b) $\overline{P_h}$, $\overline{P_\alpha}$ and $\overline{P_e}$, for an aerolastic section with 3 DOF, with piezoelectric coupling.

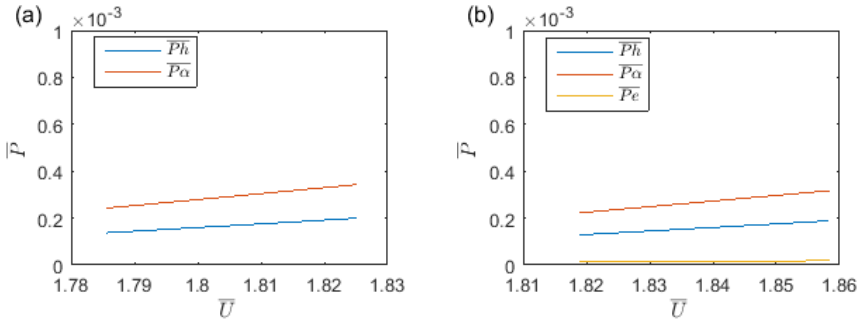

Figure 13. (a) $\overline{P_h}$ and $\overline{P_\alpha}$, for an aerolastic section with 2 DOF, without piezoelectric coupling, with nonlinear stiffness, (b) $\overline{P_h}$, $\overline{P_\alpha}$ and $\overline{P_e}$, for an aerolastic section with 3 DOF, with piezoelectric coupling, and nonlinear stiffness.

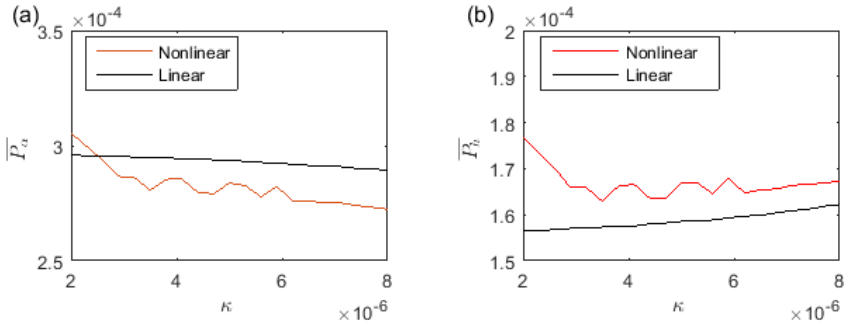

Figure 14. (a) Mechanical power related to pitch, (b) Mechanical power related to plunge.

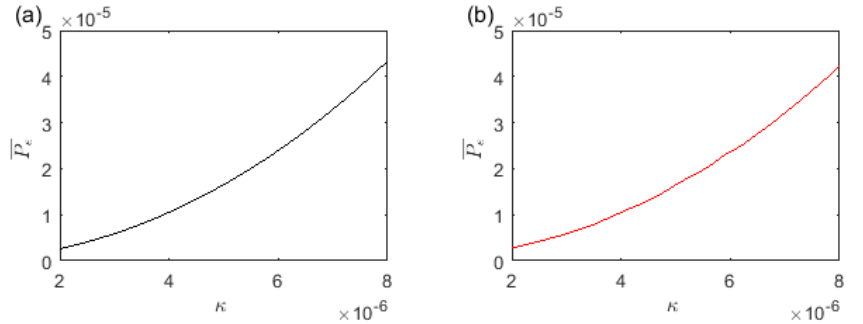

Figure 15. Electrical power as a function of the electromechanical coupling, (a) in a linear section, (b) in a nonlinear section.

of the electromechanical coupling, we have an decrease, when we compare the linear section and the nonlinear section with $\delta = 10$, from values about $\kappa = 2.5 \times 10^9$. For electrical power the nonlinearity increases in 6% the electrical power for $\kappa = 2 \times 10^{-6}$, and decreases the electrical power in 3%, for $\kappa = 8 \times 10^{-6}$.

4.2 Variation of mechanical and electrical power as a function of the electrical resistance

Figure 16 shows mechanical power related to pitch and related to plunge as a function of the electrical resistance of the system with 3 degrees of freedom (with piezoelectric), for linear section and for nonlinear section ($\delta = 10$).

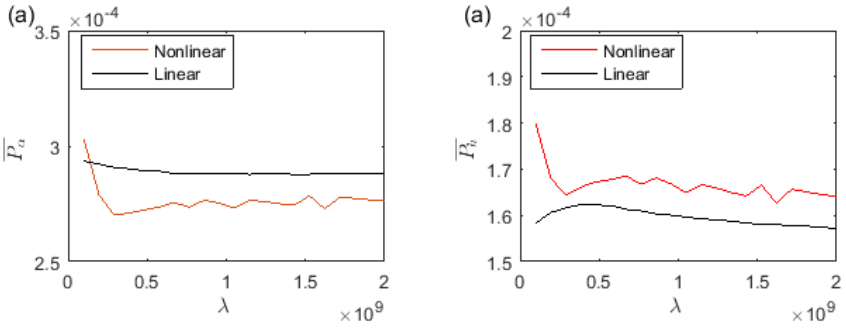

Figure 16. (a) Mechanical power related to pitch, (b) Mechanical power related to plunge.

Figure 17 shows electrical power as a function of the electrical resistance of the system with 3 degrees of freedom (with piezoelectric), for linear section and for nonlinear section ($\delta = 10$).

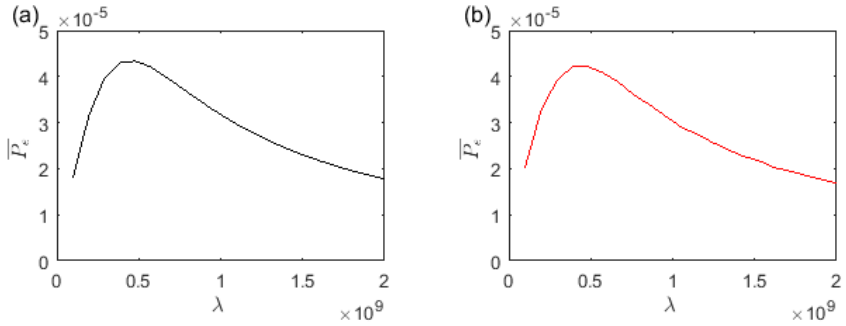

Figure 17. Electrical power as a function of electrical resistance, (a) in a linear section, (b) in a nonlinear section.

For the mechanical power related to plunge as a function of electrical resistance we have an increase when we compare the linear section and the nonlinear section with $\delta = 10$. For the mechanical power related to pitch as a function of the electrical resistance, we have an decrease, when we compare the linear section and the nonlinear section with $\delta = 10$, from values of , about $\lambda = 0.15 \times 10^9$. For electrical power the nonlinearity increases in 12.8% the electrical power for $\lambda = 0.1 \times 10^9$, and decreases the electrical power in 5.2%, for $\lambda = 2 \times 10^9$.

5. CONCLUSIONS

A two-dimensional airfoil with plunge and pitch DOFs is considered with piezoelectric coupling to the plunge displacement and included nonlinear stiffness. The linear section was studied for aerodynamic models of Edwards (1979) and of Dimitriadis (2017). The major difference between the results is given by lower values of κ, for example $\kappa = 2 \times 10^{-6}$, the difference is 0.038, for numerical solution and 0.037, for analytical solution. About piezoelectric coupling we can conclude that piezoelectric coupling increased the flutter speed of the system, consequently, it is a very interesting factor for the aeronautics, and studying the electric terms, it can be noted, that flutter speed increases, if the electromechanical coupling is increased, and for the electrical resistance, flutter speed has his maximum around 0.5×10^9. Besides that, it can be stated that the nonlinearity increases the flutter speed. About power as a function of flutter speed, the average mechanical power decreases when we put the piezoelectric in the linear case, but it increases when we put the piezoelectric in the nonlinear case. The application of nonlinearity decreases electrical power collected from energy harvesting in 0.036%, for values of $\kappa = 5 \times 10^{-6}$ and $\lambda = 0.48 \times 10^9$. At last, it was studied mechanical power related to plunge and related to pitch, and electrical power as a function of electromechanical coupling and of electrical resistance. For the mechanical power related to plunge, we have an increase when we compare the linear section and the nonlinear section with $\delta = 10$. For the mechanical power related to pitch, we have an decrease, when we compare the linear section and the nonlinear section with $\delta = 10$, from values about $\kappa = 2.5 \times 10^{-6}$, and $\lambda = 0.15 \times 10^9$. For the electrical power, the

nonlinearity increases the power for very low values of κ and λ, but decreases for other values.

6. ACKNOWLEDGEMENTS

The first author thanks CAPES (#1814902) for financial support for this project.

7. REFERENCES

Dimitriadis, G., 2017. *Introduction to Nonlinear Aeroelasticity*. John Wiley & Sons.

Edwards, J.W., 1979. "Unsteady aerodynamic modeling for arbitrary motions". *The American Institute of Aeronautics and Astronautics*, Vol. 17, pp. 365–374.

Ghandchi-Tehrani, M. and Elliott, S.J., 2014. "Extending the dynamic range of an energy harvester using nonlinear damping". *Journal of sound and vibration*, Vol. 333, pp. 623–629.

Harb, A., 2011. "Energy harvesting: State-of-the-art". *Renewable Energy*, Vol. 36, pp. 2641–2654.

Marqui Jr, C., Belo, E. and Marques, F., 2005. "A flutter suppression active controller". *Proceedings of the Institution of Mechanical Engineers, Part G: Journal of Aerospace Engineering*, Vol. 219, No. 1, pp. 19–33.

Marqui Jr, C. and Erturk, A., 2013. "Electroaeroelastic analysis of airfoil-based wind energy harvesting using piezoelectric transduction and electromagnetic induction". *Journal of Intelligent Material Systems and Structures*, Vol. 24, pp. 846–854.

Sousa, V.C., de M Anicézio, M., Jr, C.D.M. and Erturk, A., 2011. "Enhanced aeroelastic energy harvesting by exploiting combined nonlinearities: theory and experiment". *Smart Materials and Structure*, Vol. 20, p. 094007.

Sousa, V.C., Silva, T.M.P. and Marqui Jr, C., 2017. "Aeroelastic flutter enhancement by exploiting the combined use of shape memory alloys and nonlinear piezoelectric circuits". *Journal of sound and vibration*, Vol. 407, pp. 46–62.

Stephen, N.G., 2006. "On energy harvesting from ambient vibration". *Journal of sound and vibration*, Vol. 293, No. 1-2, pp. 409–425.

8. RESPONSIBILITY NOTICE

The authors are the only responsible for the printed material included in this paper.